RSC Advances

ROYAL SOCIETY OF CHEMISTRY

www.rsc.org/advances

Cu_2ZnSnS_4 Thin Film Solar Cells with 5.8 % of Conversion Efficiency Obtained by a Facile Spray Pyrolysis Technique

Thi Hiep Nguyen, Wilman Septina, Shotaro Fujikawa, Feng Jiang, Takashi Harada and Shigeru Ikeda*

Research Center for Solar Energy Chemistry, Osaka University,

1-3 Machikaneyama, Toyonaka, Osaka 560-8531, Japan

E-mail:sikeda@chem.es.osaka-u.ac.jp; Fax: +81-6-6850-6699; Tel: +81-6-6850-6696

(Tables of Contents Entry)

A CZTS-based thin film solar cell with powder conversion efficiency of 5.8% was obtained by using facile spray pyrolysis deposition followed by annealing.

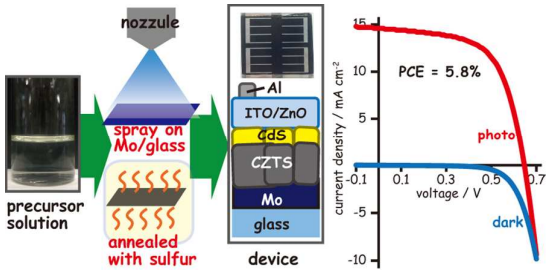

(abstract)

A attempt was made to fabricate Cu_2ZnSnS_4 (CZTS) thin film absorber on an Mo-coated glass substrate by using facile spray pyrolysis deposition of a precursor film from an aqueous solution containing $Cu(NO_3)_2$, $Zn(NO_3)_2$, $Sn(CH_3SO_3)_2$ and thiourea. In order to obtain a stable solution for the spray pyrolysis deposition without formation of an SnO_2 precipitate, the mixing order of source materials was found to be important. Annealing of the thus-obtained precursor film in a sulfur vapor at temperatures ranging from 580 ℃ to 600 °C resulted in successful formation of homogeneous films composed of CZTS crystallites. Based on structural analyses of CZTS films having different Sn contents, an Sn-rich composition compared to its stoichiometric amount was found to be essential for efficient grain growth of the resulting CZTS films. A solar cell based on the Sn-rich CZTS film obtained by an optimum annealing condition exhibited maximum conversion efficiency of 5.8%.

1. Introduction

The demand for utilization of sunlight energy has motivated many researchers to develop novel photovoltaic materials having high conversion efficiencies and/or applicable for low-cost fabrication processes. Several compound semiconductors have been used to fabricate absorber layers for thin film solar cells. Among them, kesterite compounds with chemical compositions of $Cu_2ZnSn(S,Se)_4$ (CZTSSe) are promising materials for the absorber layers of thin film solar cells because they have optimum band gap energies ranging from *ca.* 1.0 eV (for pure selenide) to *ca.* 1.5 eV (for pure sulfide) and high absorption coefficients of more than 10^4 cm^{-1}.[1-5] Moreover, these compounds do not include rare elements such as In and Ga, which are main components of the commercialized $Cu(In,Ga)(S,Se)_2$ photoabsorber. The current record power conversion efficiency (PCE) of the CZTSSe-based thin film solar cell has reached 12.6%.[6]

In view of cost effectiveness, it should be advantageous to apply non-vacuum technology for fabrication of CZTSSe thin films. Thus, various techniques, such as electrodeposition,[7-9] spin coating,[6,10-12] and spray pyrolysis[13-19] have been developed. Among them, spray pyrolysis is an attractive non-vacuum technique because of its easiness to deposit the film in a large area. Besides, composition of the films could be controlled effectively by varying the concentrations of constituents in the spray solution: as a result, films with a wide range of compositions can be prepared.[20] $Cu(In,Ga)(S,Se)_2$ solar cells with conversion efficiencies of over 10% have been obtained by this method, and the capability of this method for fabricating high quality thin-film photoabsorbers has been proven.[21,22] Some groups have reported successful fabrication of CZT(S,Se)-based thin film solar cells using the spray pyrolysis technique. For example, Zeng *et al.* prepared a CZTSSe absorber from an aqueous precursor solution of $CuCl_2$, $ZnCl_2$, $SnCl_2$, and thiourea followed by selenization.[13] They overcame the problem of instability of the spray solution by adjusting pH of the precursor solution, leading to successful formation of a uniform CZTSSe absorber layer. The solar cell based on this absorber achieved PCE of 5.1%. More recently, Khadka *et al.* prepared a cell based on a spray-deposited CZTSe-In_2S_3 heterojunction having PCE of 5.74%.[19]

Most of the CZTSSe-based solar cells reported in the literature employed CZTSSe films with selenium-rich compositions. In view of the toxicity issue, the use of pure sulfide (*i.e.*, CZTS) would be preferable. However, there have been only a few reported examples of fabrication of CZTS-based solar cells by the spray pyrolysis method; reported PECs were quite low (less than 1%),[23,24] despite several examples of successful fabrication of pure sulfide CZTS-based solar cells with high PCEs using other vacuum[25] and non-vacuum[26] techniques. These facts motivated us to prepare a highly efficient CZTS-based solar cell using the spray pyrolysis technique. In this study,

several conditions for fabricating a smooth and homogeneous CZTS film with large grain size appreciable for the absorber layer were investigated. Achievement of 5.8% PCE was demonstrated for the first time using a spray-deposited pure sulfide CZTS absorber.

2. Experimental

2.1 Fabrication of a CZTS thin film

An aqueous solution containing 0.019 M copper nitrate ($Cu(NO_3)_2$), 0.009 M zinc nitrate ($Zn(NO_3)_2$), 0.0125 M tin methanesulfonate ($Sn(CH_3SO_3)_2$) and 0.06 M thiourea ($SC(NH_2)_2$) with pH adjusted to 1.5 by adding a few drops of conc. HCl was used as a precursor solution. Eight mL of the solution was sprayed on an Mo-coated glass substrate (Mo/glass) that was heated at 380 °C using a hotplate. The as-deposited film was placed in an evacuated borosilicate glass ampoule together with 20 mg sulfur powder; the ampoule was annealed at 580-600 °C for 10-50 min. On the thus-obtained CZTS absorber film, a CdS buffer layer was deposited by chemical bath deposition (CBD).[27] An ITO/ZnO bilayer was then deposited on the top of the CdS layer by radio frequency (RF) magnetron sputtering to form a device with a structure of ITO/ZnO/CdS/CZTS/Mo/glass. In this study, active area of all the devises was fixed at 0.03 cm^2.

2.2 Characterizations

Crystalline structures of the films were analyzed by X-ray diffraction (XRD) using a Rigaku MiniFlex X-ray diffractometer (Cu Kα, Ni filter). Raman spectra were analyzed by a Jasco NRC 3100 Laser Raman Spectrophotometer with excitation laser of wavelength of 532 nm. Morphologies of the films were examined using a Hitachi S-5000 FEG field emission scanning electron microscope (SEM) at an acceleration voltage of 20 kV. Atomic compositions of the precursor solution, as-deposited films and finally obtained CZTS films were

determined by inductively coupled plasma (ICP) analysis on a Perkin-Elmer OPTIMA 3000-XL ICP emission spectrometer. For this measurement, the film samples were immersed in aqua regia overnight to dissolve all of the components. The thus-obtained clear solution was then diluted to an appropriate concentration before analysis. Current density-voltage (*J-V*) characteristics of solar cell devices under simulated AM1.5G irradiation (100 mW cm^{-2}) were determined with a Bunkoh-Keiki CEP-015 photovoltaic measurement system.

3. Results and discussion

In order to prepare an aqueous solution for spray pyrolysis, tetravalent Sn^{4+} salts such as $SnCl_4$ are unfavourable because they easily undergo hydrolysis to be precipitated even in a strongly acidic solution. Moreover, in view of its availability as a source material, the use of a divalent copper salt is better than the use of a monovalent salt, for which there is the possibility of occurrence of disproportionation or oxidation that results in loss of its chemical purity. In this work, therefore, we employed Sn^{2+} and Cu^{2+} salts as precursor materials as in the work reported by Zeng *et al*.[13] It should also be noted that care was needed in the mixing order, and appropriate content of thiourea and control of pH were indispensable to prevent precipitation induced by the oxidation of Sn^{2+} with Cu^{2+} to form an insoluble Sn^{4+} hydroxide (oxide). Indeed, when we attempted to prepare the spray solution by a mixed solution of Cu^{2+}, Sn^{2+}, and Zn^{2+} salts without addition of thiourea at uncontrolled pH as the starting solution, a white precipitate was gradually formed within a few hours, as shown in Fig. 1a. The corresponding X-ray diffraction (XRD) pattern of the precipitate indicated formation of SnO_2 (Fig. 1c). In order to overcome the problem of precipitation, therefore, it is necessary to mix Cu^{2+} and thiourea initially with a Cu^{2+}/thiourea ratio of less than 0.3. Since the divalent Cu^{2+} ion is known to be reduced by

thiourea into the monovalent Cu^{+} and the thus-formed Cu^{+} induces complexation with one or two thiourea molecules,[28.] oxidation of Sn^{2+} is inhibited. Indeed, the thus-obtained precursor solution maintained its transparency even after exposure to open air for more than 5 h, as shown in Fig. 1b.

Fig. 2 shows XRD patterns and Raman spectra of as-deposited films obtained by spray pyrolysis using the above stable precursor solution and those annealed at 580 °C and 600 °C in an evacuated glass ampoule containing sulfur powder for 10 min. As shown in Fig. 2a, the XRD pattern of the precursor film exhibited almost no diffraction peak except for peaks due to the Mo substrate, indicating that the film did not have a good crystalline nature. On the other hand, when the precursor film was annealed, the resulting film showed typical diffraction peaks corresponding to reflections derived from the kesterite CZTS.[29,30] Relatively intense and sharp peaks were observed for the film annealed at 600 °C compared to those of the film annealed at 580 °C. Indeed, full width at half maximum (FWHM) value of the most intense (112) reflection of the 600-°C annealed film (0.157) was smaller than that of the 580-°C annealed film, suggesting the achievement of a high degree of crystallinity induced by the increment of annealing temperature. It should also be noted that there are weak reflections of MoS_2 in XRD patterns of the films after annealing due to the partial sulfurization of the bottom Mo substrate (see below). Raman spectra of as-deposited film showed a significantly broad peak centered at 336 cm^{-1}, whereas the annealed films gave three separated bands at 286 cm^{-1}, 338 cm^{-1}, and 369 cm^{-1} assignable to the kesterite CZTS[31,32] without providing other signals (Fig. 2b). Hence, the annealed films obtained in this study were confirmed to form a CZTS crystal. On the other hand, since the main peak of the tetragonal Cu-Sn-S ternary compound of Cu_2SnS_3 (CTS) is present at 336 cm^{-1} and since zinc blend ZnS has a main Raman band at 351 cm^{-1},[33,34] the observed broad Raman band of the as-deposited film was likely to indicate inclusions of several less-crystalline sulfide compounds.

Fig. 3 shows cross-sectional and surface SEM images of an as-deposited film and CZTS films obtained at different annealing temperatures and durations. The as-deposited film was composed of densely packed small granule particles with a thickness of more than 1 μm, indicating successful deposition of a homogeneous film (Fig. 3a). The annealing treatment induced appreciable grain growth without alteration of thicknesses when compared to that of the as-deposited film. As expected from the above XRD results, the film annealed at 600 °C showed larger grain sizes than those of the film annealed at 580 °C (Figs. 3b and 3c). Another point worth noting is that dark regions on the upper part of the Mo substrate are attributed to formation of MoS_2, as confirmed by the above XRD analyses.

Although formation of well-grown CZTS grains seemed to be achieved by the annealing at 600 °C, the corresponding surface SEM image shown in Figs. 3c and 3d indicated incomplete grain growth and thereby a more severe annealing condition would be required. Due to the limitation of the thermal stability of the glass substrate, however, annealing temperature could not be increased to a temperature over 600 °C. Therefore, the annealing duration was extended for 30 min and 50 min to accelerate the grain growth of CZTS. Figs. 3e-3h show cross-sectional and surface SEM images of thus-obtained CZTS films. As we expected, clear micron-sized grains were observed in their surface images. XRD analyses of those films (Fig. S1) showed narrower FWHMs (0.151 and 0.143 for 30-min and 50-min annealed films, respectively) than that of the 10-min annealed film (see above) in agreement with the SEM results. Dense morphologies of these films were seemed to be favorable for photovoltaic application. Corresponding cross-sections also showed densely packed large grains: however, sulfurization of the Mo layer advanced compared to that of the film annealed at the short duration (10 min, as shown in Fig. 3c). Specifically for the film obtained by 50-min annealing, most parts of the Mo substrate had sulfurized into MoS_2. The thick

MoS_2 should affect the device performance because of induction of an increase in series resistance, as discussed below.

ICP measurements were performed to determine metallic compositions of the as-deposited film and the film annealed at 600 ℃ for 30 min. Because of the deliquescent nature of the copper source ($Cu(NO_3)_2$) used, accurate composition of the precursor solution was also determined by ICP analysis. Table 1 summarizes the results. When compared to the stoichiometric composition, the precursor solution used contained excess amounts of the Sn component, whereas both Cu and Zn components were close to their stoichiometry. A notable feature is that the Sn content was reduced significantly in the as-deposited film, while the film annealed at 600 °C still had an Sn-rich composition. The loss of Sn indicated the occurrence of evaporation during the spray pyrolysis deposition even at ambient pressure. One of the possible explanations is formation of tin monosulfide (SnS) because of its low vapor pressure.[35-37] Since the as-deposited film did not form CZTS crystallite and other sulfides containing a smaller amount of Sn (CTS) and without Sn (ZnS), a highly Sn-rich composition is likely to be indispensable to compensate for a shortage induced by evaporation. Regarding the composition of the final CZTS film obtained by annealing at 600 °C for 30 min, the Sn content was slightly reduced but still Sn-rich compared to its stoichiometry. The annealing was performed in an evacuated glass ampoule containing sulfur vapor (see experimental). Thus, loss of the Sn component was suppressed even though the temperature was elevated to a temperature higher than that of spray deposition.

The literature work indicated that both Cu-poor and Zn-rich compositions from the stoichiometric composition were indispensable to obtain an efficient absorber for photovoltaic applications.[38] Although the CZTS film obtained in this study was not such an empirical optimum, use of the composition, at least the Sn-rich composition, was found to be advantageous for grain growth. In fact, when precursor solutions containing relatively small amounts of Sn (*i.e.*, close to

its stoichiometry and Sn-poor relative to Cu and Zn) were used, final CZTS films obtained by annealing at 600 °C were composed of small grains with less compact morphologies, as shown in Fig. 4. Based on the fact that appreciable grain growth could be achieved by using SnS vapor during a high temperature (550 °C) annealing process as reported by Toyama *et al.*,[39] the excess Sn component in the as-deposited film would have a similar function in the present annealing performed in the evacuated glass ampoule.

Solar cells with a device structure of ITO/ZnO/CdS/CZTS/Mo/glass (without an antireflection coating) were prepared by deposition of CdS, ZnO, and ITO layers on CTZS films obtained by annealing at 600 °C for 10 min, 30 min, and 50 min. From the measurements of device properties for the three samples, all of the devices exhibited solar cell performance with good productivity (Fig. S1). Fig. 5 shows the best *J-V* curves of these devices based on the CZTS films obtained by annealing at 600 °C for different durations under irradiation of simulated sunlight (AM1.5G) together with their corresponding semi-logarithmic dark *J-V* characteristics. Short-circuit current density (J_{SC}), open circuit voltage (V_{OC}), fill factor (FF) and PCE of these cells were determined from the illuminated *J-V* curves. These cell parameters are summarized in Table 2. The best performance with PCE of 5.8% was achieved by the device made from the 30-min annealed CZTS (DEV30), whereas appreciable drops in all of the solar cell parameters were observed for the device based on the 10-min annealed CZTS (DEV10); further reduction of solar cell parameters, especially J_{SC}, appeared in the device composed of the 50-min annealed CZTS film (DEV50). Compared to the *J-V* characteristic of the best device of DEV30, the best device of DEV10 showed poor electrical rectification with a significantly low FF value, as shown in Fig. 5a. The relatively gentle slope of the J-V curve of DEV10 at the X-intersect compared to that of DEV30 suggests a large series resistance (R_s) of the DEV10 device. As discussed above SEM results of CZTS films employed for these devices, the large R_s of DEV10 is likely to be derived from

incomplete crystallization of CZTS grains. Regarding dark *J-V* curves of DEV10 and DEV30 devices shown in Fig. 5b, appreciable differences were also observed in both negative and positive bias regions. In the former negative bias region, a relatively strong current was observed for DEV10 compared to that for DEV30, indicating the presence of appreciable shunts in the DEV10 device. In the latter positive bias region (at *ca.* 0.2-0.6 V), DEV10 also showed an appreciably large dark current relative to that of DEV30. The result suggests presences of appreciable recombination currents in addition to diffusion currents in the device due probably to the poor quality of the p-n junction (i.e., presences of appreciable amounts of defects at the CZTS-CdS interface. Therefore, these poor device properties of DEV10 are attributable to incomplete crystallization of the CZTS grains as well as significant amounts of defects at the CZTS-CdS junction. On the other hand, the dark *J-V* curve of DEV50 showed a different characteristic, *i.e.*, it showed a weak current flow at the highly positive bias region (> *ca.* 0.6 V) even though it gave better rectification than that of DEV10. Considering the above cross-sectional SEM results for the 50-min annealed film (see Fig. 3g), the observed weak currents were derived from the presence of a thick MoS_2 layer, leading to a large series resistance of the device. Due to less structural failures of the DEV30 device, it gave the best efficiency in the present study.

Fig. 6 shows the external quantum efficiency (EQE) spectrum of the best device (DEV 30) in wavelengths ranging from 300 nm to 1000 nm. It can be seen that the spectrum increases gradually from ca. 370 nm to ca. 500 nm and rapidly increases to ca. 540 nm; and then gradually degreases from ca. 700 nm to the onset wavelength of ca. 900 nm. The loss in the spectrum in the short wavelength was attributed to absorption losses in the buffer CdS layers. Meanwhile, the loss in the long wavelength region indicated loss of deeply absorbed photons due to poor minority carrier diffusion length and/or insufficient penetration of depletion width into the absorber. Such structural failures led to insufficient solar cell parameters (specifically J_{SC}) when compared to the

efficient CZTS-based solar cells reported in the literature.[25,26] The optimization of the deposition condition of the CdS buffer layer to reduce its thickness or the use of an alternative buffer layer should reduce the loss in the short wavelength region. Moreover, as mentioned above, successful fabrication of a CZTS film having an empirical optimum composition would be one of the most significant key structures to be achieved in order to obtain a high quality CZTS film without a significant loss in the long wavelength region. Hence, studies along these lines are now in progress.

4. Conclusions

In this study, we fabricated a CZTS thin film-based solar cell by using a facile spray pyrolysis technique. Successful grain growth of the CZTS absorber was achieved by employing an Sn-rich composition of the precursor solution with application of adequate post annealing at a high temperature (600 °C) for a sufficient duration (30 min). The solar cell based on the thus-obtained CZTS absorber reached PCE of 5.8%. To the best of our knowledge, this value is the best value so far reported for a pure-sulfide CZTS-based device obtained through spray deposition of the CZTS film. Concerning the chemical composition of the CZTS film, the performance of the present solar cell can be improved by its optimization to achieve a Cu-poor and Zn-rich composition as reported in the literature. Moreover, since the present spray technique enables easy control of the chemical composition by just changing the concentration of the precursor solution, it is also possible to add other beneficial components such as sodium and potassium.[40-42] Hence, we can expect further improvement of PEC after optimizations of such compositional properties of the CTZS film as well as various modifications of device structures.

Acknowledgements

This work was supported by a Grant-in-Aid for Scientific Research on Innovative Areas (All Nippon Artificial Photosynthesis Project for Living Earth) and a Grant-in-Aid for Scientific Research (B) from MEXT Japan. This work was also carried out as a part of the A-step feasibility study program from JST Japan. One of the authors (Thi Hiep Nguyen) would like to thank MEXT for providing a scholarship during the study.

Notes and references

1 H. Katagiri, *Thin Solids Films*, 2005, **480-482**, 426-432.

2 A. H. Reshak, K. Nouneh, I. V. Kityk, J. Bila, S. Auluck, H. Kamarudin and Z. Sekkat, *Int. J. Electrochem. Sci.*, 2014, **9**, 955-974.

3 X. Lin, J. Kavalakkatt, K. kornhuber, S. Levcenko, M. C. L. Steiner and A. Ennaoui, *Thin Solid Films*, 2013, **535**, 10-13.

4 J. Krustok, R. Josepson, T. Raadik and M. Danilson, *Physica B*, 2010, **405**, 3186-3189.

5 G. Larramona, S. Bourdais, A. Jacob, C. Chone, T. Muto, Y. Cuccaro, B. Delatouche, C. Moisan, D. Pere and G. Dennler, *J. Phys. Chem. Lett.*, 2014, **5**, 3763-3767.

6 W. Wang, M. T. Winkler, O. Gunawan, T. Gokmen, T. K. Todorov, Y. Zhu and D. B. Mitzi, *Adv. Energy Mater.*, 2014, **4**, 1301465.

7 H. Chen, Q. Ye, X. He, J. Ding, Y. Zhang, J. Han, J. Liu, C. Liao, J. Mei and W. Lau, *Green Chem.*, 2014, **16**, 3841-3845.

8 J. O. Jeon, K. D. Lee, L. S. Oh, S. W. Seo, D. K. Lee, H. Kim, J. H. Jeong, M. J. Ko, B. S. Kim, H. J. Son and J. Y. Kim, *ChemSusChem*, 2014, **7**, 1073-1077.

9 M. I. Khalil, R. Bernasconi and L. Magagnin, *Electrochimica Acta*, 2014, **145**, 154-158.

10 K. D. Zhang, Z. R. Tian, J. B. Wang, B. Li, X. L. Zhong, D. Y. Guo and S. M. He, *J. Sol-Gel Sci. Technol.*, 2015, **73**, 452-459.

11 J. Wang, P. Zhang, X. Song and L. Gao, *RSC Adv.*, 2014, **4**, 21318-21324.

12 S. K. Swami, A. Kumar and V. Dutta, *Energy Procedia*, 2013, **33**, 198-202.

13 X. Zeng, K. F. Tai, T. Zhang, C. W. J. Ho, X. Chen, A. Huan, T. C. Sum and L. H. Wong, *Sol. Energy Mater. Sol. Cells*, 2014, **124**, 55-60.

14 M. Valdes, G. Santoro and M. Vazquez, *J. Alloys and Compd.*, 2014, **585**, 776-782.

15 N. M. Shinde, R. J. Deokate and C. D. Lokhande, *J. Anal. Appl. Pyrolysis*, 2013, **100**, 12-16.

16 Y. B. K. Kumar. P. U. Bhaskar, G. S. Babu, S. Raja, *phys. stat. solidi A*, 2010, **207**, 149-156.

17 M. Patel, I. Mukhopadhyay and A. Ray, *J. Phys. D: Appl. Phys.*, 2012, **45**, 445103.

18 Y. B. K. Kumar, G. S. Babu, P. U, Bhaskar and V. S, Raja, *Sol. Energy Mater. Sol. Cells*, 2009, **93**, 1230-1237.

19 D. B. Khadka, S. Y. Kim and J. H. Kim, *J. Phys. Chem. C*, 2015, **119**, 12226-12235.

20 S. Ikeda, M. Nonogaki, W. Septina, G. Gunawan, T. Harada and M. Matsumura, *Catal. Sci. Technol.*, 2013, **3**, 1849-1854.

21 W. Septina, M. Kurihara, S. Ikeda, Y. Nakajima, T. Hirano, Y. Kawasaki, T. Harada and M. Matsumura, *ACS Appl. Mater. Interfaces*, 2015, **7**, 6472-6479.

22 M. A. Hossain, Z. Tianliang, L. K. Keat, L. Xianglin, R. R. Prabhakar, S. K. Batabyal, S. G. Mhaisalkar and L. H. Wong, *J. Mater. Chem. A*, 2015, **3**, 4147-4154.

23 O. V. Galan, M. Courel, M. E. Rodriguez, V. I. Roca, E. Saucedo, A. Fairbrother, *J. Renewable Sustainable Energy,* 2013, **5**, 053137.

24 M. E. Rodriguez, M. Placidi, O. V. Galan, V. I. Roca, X. Fontane, A. Fairbrother, D. Sylla, E. Saucedo and A. P. Rodriguez, *Thin Solid Films*, 2013, **535**, 67-72.

25 B. Shin, O. Gunawan, Y. Zhu, N. A. Bojarczuk, S. J. Chey and S. Guha, *Prog. Photovolt: Res. Appl.,* 2013, **21**, 72-76.

26 F. Jiang, S. Ikeda, T. Harada and M. Matsumura, *Adv. Energy Mater*., 2014, **4**, 1301381.

27 S. Ikeda, R. Kamai, T. Yagi and Michio Matsumura, *Journal of The Electrochemical Society*, 2010, **157**, B99-B103.

28 G. A. Bowmaker, J. V. Hanna, C. Pakawatchai, B. W. Skelton, Y. Thanyasirikul and A. H. White, *Inorg. Chem*., 2009, **48**, 350-368.

29 J. W. Cho, A. Ismail, S. J. Park, W. Kim, S. Yoon and B. K. Min, *Appl. Mater. Interfaces*, 2013, **5**, 4162-4165.

30 Z. Su, K. Sun, Z. Han, H. Cui, F. Liu, Y. Lai, J. Li, X. Hao, Y. Liu and M. A. Green, *J. Mater. Chem. A*, 2014, **2**, 500-509.

31 S. K. Swami, N. Chaturvedi, A. Kumar, N. Chander, V. Dutta, D. K. Kumar, A. Ivaturi, S. Senthilarasu and H. M. Upadhyaya, *Phys. Chem. Chem. Phys.*, 2014, **16**, 23993-23999.

32 Z. Li, J. C. W. Ho, K. K. Lee, X. Zeng, T. Zhang, L. H. Wong and Y. M. Lam, *RSC Adv.*, 2014, **4**, 26888-26894.

33 P. A. Fernandes, P. M. P. Salomé and A. F. da Cunha, *phys. stat. solidi c*, 2010, 7, 901-904.

34 Y. C. Cheng, C. Q. Jin, F. Gao, X. L. Wu, W. Zhong, S. H. Li and P. K. Chu, *J. Appl. Phys.*, 2009, **106**, 123505.

35 C. P. Bjorkman, J. Scragg, H. Flammersberger, T. Kubart and M. Edoff, *Sol. Energy Mater. Sol. Cells*, 2012, **98**, 110-117.

36 M. Cao, L. Li, B. L. Zhang, J. Huang, L. J. Wang, Y. Shen, Y. Sun and J. C. Jiang, *Sol. Energy Mater. Sol. Cells*, 2013, **117**, 81-86.

37 A. Weber, R. Mainz and H. W. Schock, *J. Appl. Phys.*, 2010, **107**, 013516.

38 H. Katagiri , K. Jimbo, M. Tahara, H. Araki, K. Oishi,, in Thin-Film Compound Semiconductor Photovoltaics 2009 (A Yamada, C. Heske, M.Contreras, M. Igalson, S. J.C. Irvine (Eds.)), *Mater. Res. Soc. Symp. Proc.*, 2009, 1165-M04-01.

39 T. Toyama, T. Konishi, Y. Seo, R. Tsuji, K. Terai, Y. Nakashima, H. Okamoto and Y. Tsutsumi, *Appl. Phys. Express,* 2013, **6**, 075503.

40 J. V. Li, D. Kuciauskas, M. R. Young and I. L. Repins, *Appl. Phys. Lett.*, 2013, **102**, 163905.

41 M. Johnson, S. V. Baryshev, E. Thimsen, M. Manno, X. Zhang, I. V. Veryovkin, C. Leighton and E. S. Aydil, *Energy Environ. Sci*., 2014, **7**, 1931-1938.

42 P. Salome, V. Fjallstrom, A. Hultqvist and M. Edoff, *IEEE Journal of Photovoltaics*, 2013, **3**, 509-513.

Figure Captions

Fig. 1 Photographs of (a) an aqueous solution containing Cu^{2+}, Sn^{2+}, and Zn^{2+} salts after leaving for 4 h in an ambient condition and (b) the spray solution used in this study after exposure to an open air for 8 h. (c) An XRD pattern of the white precipitate collected from the solution containing Cu^{2+}, Sn^{2+}, and Zn^{2+} salts.

Fig. 2 (Upper) XRD patterns and (lower) Raman spectra of (a) the as-deposited film and the film annealed (b) at 580 °C for 10 min and (c) at 600 °C for 10 min.

Fig. 3 Cross-sectional and surface SEM images of (a) as-deposited film and CZTS films obtained by annealing the as-deposited film (b) at 580 °C for 10 min, (c,d) at 600 °C for 10 min, (e,f) at 600 °C for 30 min, and (g,h) at 600 °C for 50 min.

Fig. 4. Surface SEM images of CZTS films obtained by annealing the as-deposited film at 600 °C for 30 min. (a) The film was derived from a precursor solution containing almost stoichiometric amounts of Sn^{2+} salt. (b) The film was obtained by using a precursor solution having a slightly Sn-poor composition relative to the stoichiometry of metallic components in CZTS.

Fig. 5 *J-V* characteristics of ITO/ZnO/CdS/CZTS/Mo/glass solar cells. These devices were made from CZTS films obtained by annealing the as-deposited film at 600 °C for (a) 10 min, (b) 30 min, and (c) 50 min. Upper: under simulated AM1.5G irradiation; lower: in the dark (on a semi-logarithmic scale).

Fig. 6. An EQE spectrum of the device made from CZTS film obtained by annealing the as-deposited film at 600 °C for 30 min.

Table 1 Metallic compositions of the precursor solution, as-deposited film on an Mo/glass, and the film annealed at 600 °C for 30 min in an evacuated glass ampoule containing sulfur powder

Sample	Metal content ratio			Cu/Sn ratio	Cu/Zn ratio
	Cu	Sn	Zn		
Precursor[a]	0.34	0.49	0.17	0.7	2.0
As-deposited[b]	0.49	0.27	0.23	1.8	2.1
Annealed[c]	0.49	0.26	0.25	1.9	2.0
(stoichiometry)[d]	0.50	0.25	0.25	2.0	2.0

[a] Precursor solution. [b] As-deposited film obtained by the spray pyrolysis deposition. [c] The CZTS film obtained by annealing the as-deposited film at 600 °C for 30 min. [d] Ideal composition of metallic components in the stoichiometric CZTS compound.

Table 2 Solar cell parameters of solar cells made from CZTS films obtained by annealing of the as-deposited film at 600 °C for different durations

Annealing duration[a] / min	J_{SC} /mA cm^{-2}	V_{OC}/mV	FF	PCE (%)
10	11.1	534	0.44	2.8
30	14.6	647	0.61	5.8
50	4.2	531	0.40	0.9

[a] Duration of annealing of the as-deposited film at 600 °C.

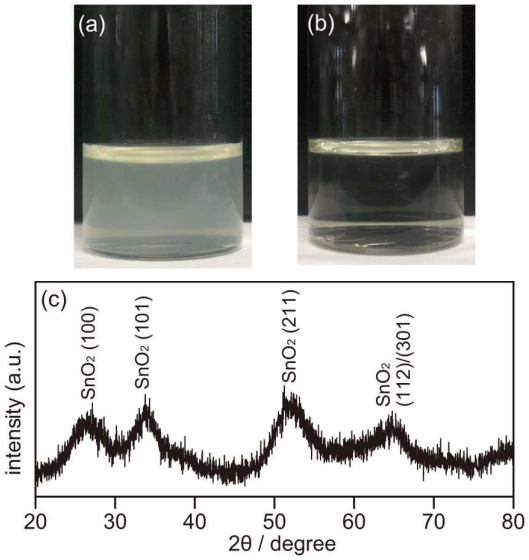

Fig. 1

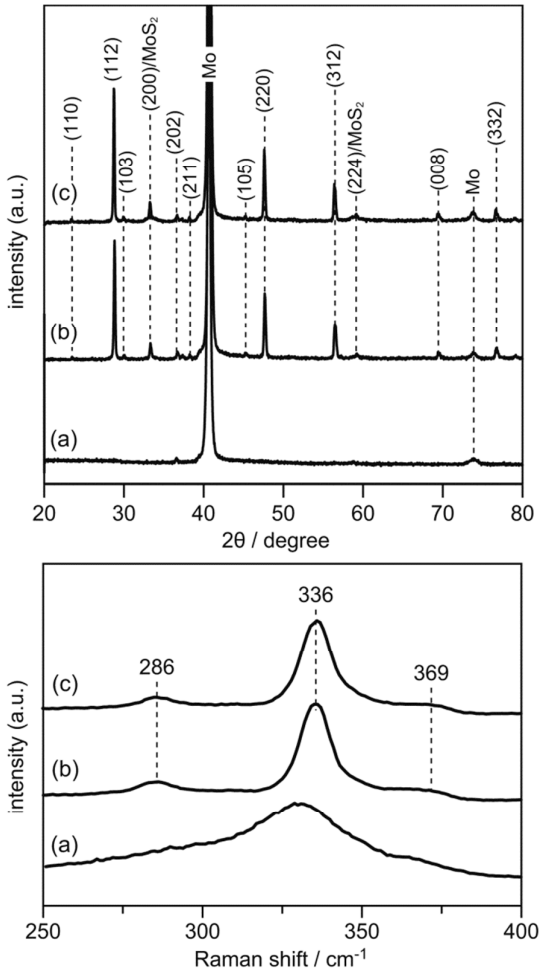

Fig. 2

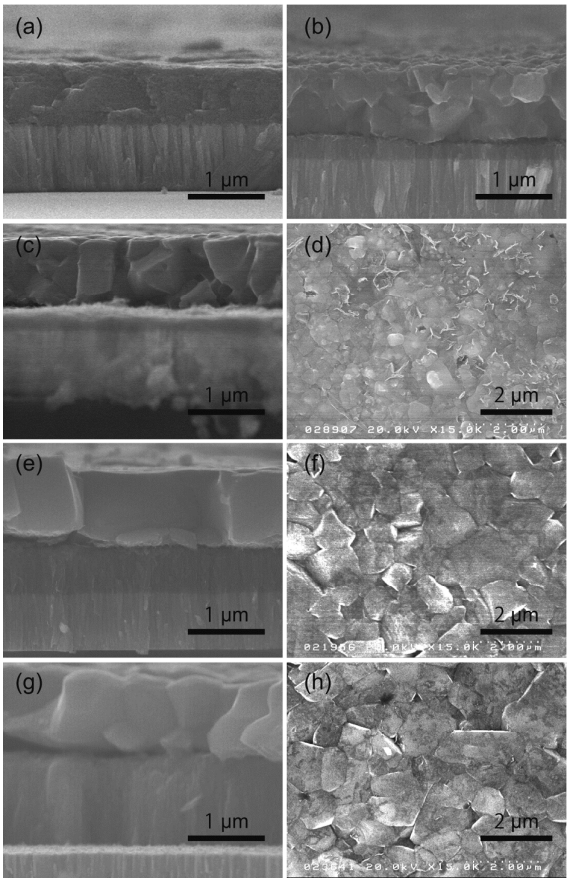

Fig. 3

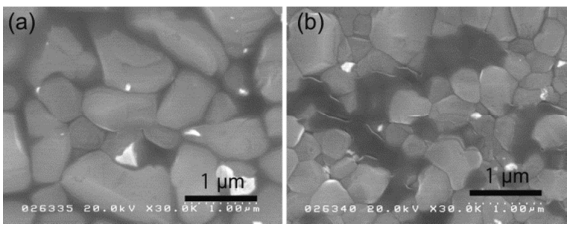

Fig. 4

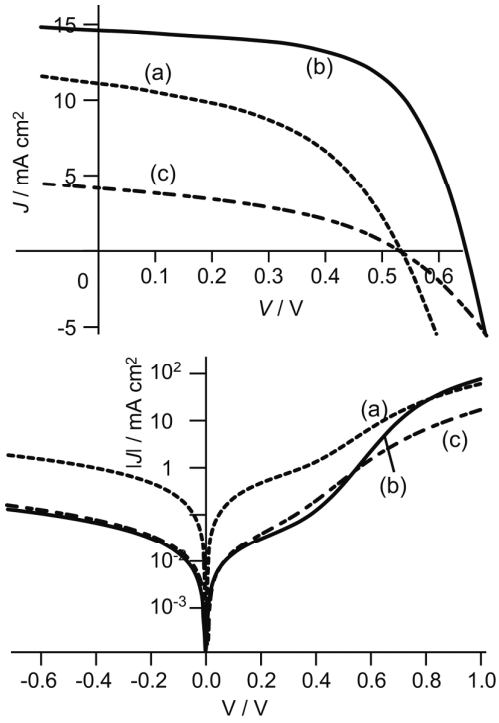

Fig. 5

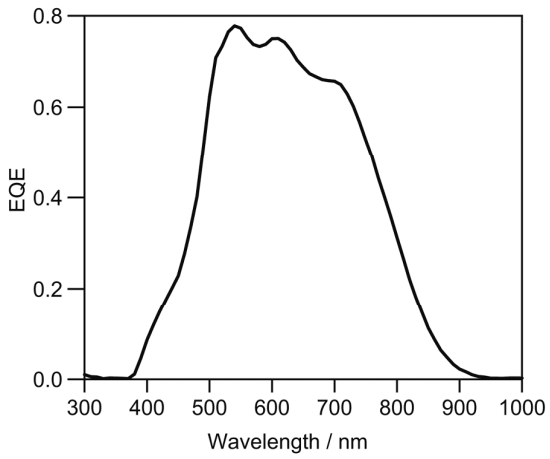

Fig. 6